

Mechanism of Glucose Oxidation by Quinoprotein Soluble Glucose Dehydrogenase: Insights from Molecular Dynamics Studies

Swarnalatha Y. Reddy and Thomas C. Bruice*

Contribution from the Department of Chemistry and Biochemistry, University of California, Santa Barbara, California 93106

Received November 20, 2003; E-mail: tcbuice@chem.ucsb.edu

Abstract: We have generated 3 ns molecular dynamic (MD) simulations, in aqueous solution, of the bacterial soluble glucose dehydrogenase *enzyme-PQQ-glucose* complex and intermediates formed in PQQ reduction. In the MD structure of *enzyme-PQQ-glucose* complex the imidazole of His144 is hydrogen bonded to the hydroxyl hydrogen of H-OC1(H) of glucose. The tightly hydrogen-bonded triad Asp163-His144-glucose (2.70 and 2.91 Å) is involved in proton abstraction from glucose concerted with the hydride transfer from the C1-H of glucose to the >C5=O quinone carbon of PQQ. The reaction is assisted by Arg228 hydrogen bonding to the carbonyl oxygen of >C5=O. The rearrangement of -(H)C5(O⁻)-C4(=O)- of II to -C5(OH)=C4(OH)- of PQQH₂ hydroquinone is assisted by general acid protonation of the >C4=O oxygen by protonated His144 and hydrogen bonds of Arg228 to the oxyanion O5. The continuous hydrogen bonding of the amide side chain of Asn229 to >C4=O oxygen and that of the O5 oxygen of the cofactor to Wat89 is observed throughout the entire reaction.

Introduction

The bacterial glucose dehydrogenase (GDH) enzymes belong to the family of quinoproteins, in which PQQ (2,7,9-tricarboxy-1H-pyrrolo [2,3-f]-quinoline-4,5-dione) is cofactor.¹⁻⁴ Two GDHs that are completely different in their amino acid sequences have been identified in *Acinetobacter calcoaceticus*.^{5,6} One is a cytoplasmic membrane-bound enzyme⁷ (mGDH), which is also present in many other Gram-negative bacteria, and the other, a soluble enzyme, sGDH. Similar to the quinoprotein methanol dehydrogenase (MDH), GDH requires Ca²⁺ for catalytic activity.^{8,9} GDH is a respiratory chain-linked enzyme that oxidizes a wide range of pentose and hexose sugars to their corresponding lactones, with concomitant reduction of PQQ coenzyme.

The subject of this study is sGDH a basic (pI = 9.5) dimeric enzyme (Figure 1) with identical subunits with molecular weight of 50 kDa (452 residues).^{3,5} Each monomer has a β -propellor fold with six four-stranded antiparallel β -sheets. Two mechanisms, similar to those proposed for the alcohol oxidizing enzyme, MDH have been suggested for sGDH catalysis. The first (Scheme 1) involves a general base-catalyzed proton

abstraction from the substrate glucose in concert with direct hydride transfer (or equivalent) from glucose to the quinone carbonyl carbon, C5 of PQQ and subsequent tautomerization to the hydroquinone PQQH₂.^{10,11} The second mechanism involves the nucleophilic addition by O1 oxygen of glucose to the carbonyl C5 of PQQ.^{10,12} From X-ray coordinates it has been concluded that the energetically expensive addition-elimination mechanism is unlikely. Also, support for the hydride-transfer or equivalent mechanism has been presented on the basis of the determined anomer selectivity of the enzyme for β -D-glucose.^{11,13,14} The reduced enzyme product complex (sGDH·PQQH₂), is subject to 1e⁻ oxidation by a number of reagents,^{8,15} including a soluble cytochrome *b*₅₆₂.¹⁶ The physiological electron acceptor of sGDH is unknown. Kinetic studies of sGDH establish a pH optimum of around 7.0¹⁰ and a high turnover number.¹⁵

X-ray structures assigned to apo-sGDH,¹⁷ sGDH·PQQH₂, and sGDH·PQQH₂·glucose are available.¹¹ Details of the enzymatic redox mechanism are not clear. We describe herein molecular dynamics (MD) studies of the ground state (sGDH·PQQ·glucose) and intermediate structures of the hydride-transfer

- (1) Hauge, J. G. *J. Biol. Chem.* **1964**, 239, 3630.
- (2) Duine, J. A.; Frank, J.; van Zeeland, J. K. *FEBS Lett.* **1979**, 108, 443.
- (3) Dokter, P.; Frank, J. J.; Duine, J. A. *Biochem. J.* **1986**, 239, 163.
- (4) Geiger, O.; Gorisch, H. *Biochemistry* **1986**, 25, 6043.
- (5) Cleton-Jansen, A.-M.; Goosen, N.; Wenzel, T. J.; van de Putte, P. *J. Bacteriol.* **1988**, 170, 2121.
- (6) Matsushita, K.; Shinagawa, E.; Adachi, O.; Ameyama, M. *Biochemistry* **1989**, 28, 6276.
- (7) Matsushita, K.; Shinagawa, E.; Inoue, T.; Adachi, O.; Ameyama, M. *FEMS Microbiol. Lett.* **1986**, 37, 141.
- (8) Olsthoorn, A. J. J.; Duine, J. A. *Arch. Biochem. Biophys.* **1996**, 336, 42.
- (9) Olsthoorn, A. J. J.; Otsuki, T.; Duine, J. A. *Eur. J. Biochem.* **1997**, 247, 659.

- (10) Olsthoorn, A. J. J.; Duine, J. A. *Biochemistry* **1998**, 37, 13854.
- (11) Oubrie, A.; Rozeboom, H. J.; Kalk, K. H.; Olsthoorn, A. J. J.; Duine, J. A.; Dijkstra, B. W. *EMBO J.* **1999**, 18, 5187.
- (12) Oubrie, A.; Rozeboom, H. J.; Dijkstra, B. W. *Proc. Natl. Acad. Sci. U.S.A.* **1999**, 96, 319.
- (13) Oubrie, A.; Dijkstra, B. W. *Protein Sci.* **2000**, 9, 1265.
- (14) Dewanti, A. R.; Duine, J. A. *Biochemistry* **2000**, 39, 9384.
- (15) Ye, L.; Hammeric, M.; Olsthoorn, A. J. J.; Schuhmann, W.; Schmidh, H. L.; Duine, J. A. *Anal. Chem.* **1993**, 65, 238.
- (16) Dokter, P.; van Wielink, J. E.; van Kleef, M., A.; Duine, J. A. *Biochem. J.* **1988**, 254, 131.
- (17) Oubrie, A.; Rozeboom, H. J.; Kalk, K. H.; Duine, J. A.; Dijkstra, B. W. *J. Mol. Biol.* **1999**, 289, 319.

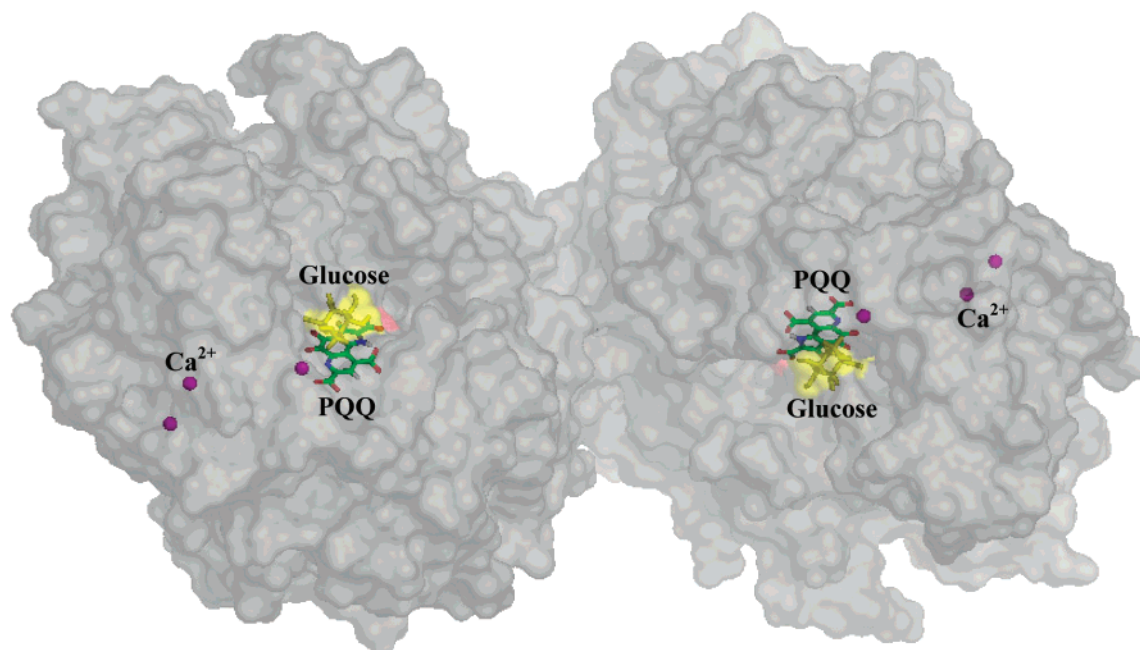


Figure 1. Molecular surface of the dimeric enzyme, soluble glucose dehydrogenase with the cofactor PQQ and substrate glucose (yellow), in stick representation, in each subunit. Notice the three Ca^{2+} ions (magenta), with one of them in the active site of each subunit.

Scheme 1

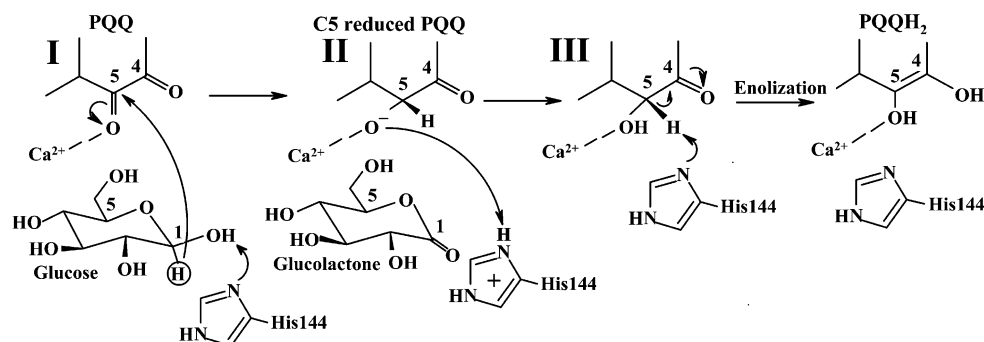
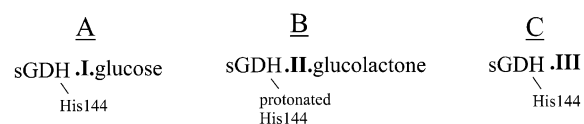


Chart 1



mechanism (sGDH·II·glucolactone and sGDH·III of Scheme 1). These structures referred to as **A**, **B**, and **C** are given in Chart 1.

Methods

The starting homodimer structure (1.9 Å resolution) of sGDH·PQQ·glucose was taken from the entry 1CQ1 of the Protein Data Bank.¹¹ The partial atomic charges of the PQQ in the presence of the Ca^{2+} ion were obtained by means of quantum chemical calculations using Gaussian 98.¹⁸ The PQQ structure with 2,7,9-tricarboxyl functions ionized was optimized at the HF/6-31+G(d,p) level. The electrostatic potential was calculated at the MP2/6-31+G(d,p) level using the Merz–Singh–Kollman scheme.¹⁹ The restrained electrostatic potential (RESP) method²⁰ was used to fit the electrostatic potential using an atom-centered point-charge model. Similar procedures were adopted to obtain the partial charges of the C5 reduced intermediates of PQQ (**II** and **III**, respectively of Scheme 1) and also the product, glucolactone.

Hydrogen atoms were added to the crystal structure¹¹ using the program CHARMM²¹ (version c27b4) and CHARMM27 all-atom force

field parameters.²² The protonation sites of the histidines of sGDH were based on the availability of proximal hydrogen bond donors and acceptors. Due to the suggested role of the His144 in the oxidation of glucose,¹¹ His144 was protonated in both the subunits of structure **B**. To neutralize the total charge of the enzyme, Cl^- ions were placed at a distance of 3.0 Å near the side chains of solvent-exposed Lys and

- (18) Frisch, M. J.; Trucks, G. W.; Schlegel, H. B.; Scuseria, G. E.; Robb, M. A.; Cheeseman, J. R.; Zakrzewski, V. G.; Montgomery, J. A., Jr.; Stratmann, R. E.; Burant, J. C.; Dapprich, S.; Millam, J. M.; Daniels, A. D.; Kudin, K. N.; Strain, M. C.; Farkas, O.; Tomasi, J.; Barone, V.; Cossi, M.; Cammi, R.; Mennucci, B.; Pomelli, C.; Adamo, C.; Clifford, S.; Ochterski, J.; Petersson, G. A.; Ayala, P. Y.; Cui, Q.; Morokuma, K.; Malick, D. K.; Rabuck, A. D.; Raghavachari, K.; Foresman, J. B.; Cioslowski, J.; Ortiz, J. V.; Stefanov, B. B.; Liu, G.; Liashenko, A.; Piskorz, P.; Komaromi, I.; Gomperts, R.; Martin, R. L.; Fox, D. J.; Keith, T.; Al-Laham, M. A.; Peng, C. Y.; Nanayakkara, A.; Gonzalez, C.; Challacombe, M.; Gill, P. M. W.; Johnson, B.; Chen, W.; Wong, M. W.; Andres, J. L.; Gonzalez, C.; Head-Gordon, M.; Replogle, E. S.; Pople, J. A. *Gaussian 98*, version A.6; Gaussian Inc.: Pittsburgh, PA, 1998.
- (19) Besler, B. H.; Merz, K. M.; Kollman, P. A. *J. Comput. Chem.* **1990**, *11*, 431.
- (20) Bayly, C. I.; Cieplak, P.; Cornell, W. D.; Kollman, P. A. *J. Phys. Chem.* **1993**, *97*, 10269.
- (21) Brooks, B. R.; Bruccoleri, R. E.; Olason, B. D.; States, D. J.; Swaminathan, S.; Karplus, M. *J. Comput. Chem.* **1983**, *4*, 187.
- (22) MacKerell, A. D., Jr.; Bashford, D.; Bellott, M.; Dunbrack, J. R. L.; Evanseck, J. D.; Field, M. J.; Fischer, S.; Gao, J.; Guo, H.; Ha, S.; Joseph-McCarthy, D.; Kuchnir, L.; Kuczera, K.; Lau, F. T. K.; Mattos, C.; Michnick, S.; Ngo, T.; Nguyen, D. T.; Prodhom, B.; Reiher, W. E., III; Roux, B.; Schlenkerich, M.; Smith, J. C.; Stote, R.; Straub, J.; Watanabe, M.; Wiorkiewicz-Kuczera, J.; Yin, D.; Karplus, M. *J. Phys. Chem. B* **1998**, *102*, 3586.

Arg residues. Each structure with 600 crystal waters was minimized for 500 steps of steepest descent (SD) and 1500 steps of adopted basis Newton–Raphson (ABNR) methods.

The structures **A**, **B**, and **C** were solvated in an equilibrated TIP3P²³ water sphere of 42 Å radius using the center of mass of the cofactor bound to subunit A as the origin. Solvent molecules within 2.8 Å of heavy atoms were deleted. The solvated system contains the whole of subunit A and parts of subunit B. The structure **A** has a total of 35,243 atoms, and the intermediate complexes **B** and **C** contain 35,270 and 35,259 atoms, respectively. Positions of water molecules were minimized for 200 steps of SD followed by 2000 steps of ABNR methods in each structure, keeping the ions and enzyme complex or intermediate fixed. Later, the entire structure was minimized for 200 steps of SD and 2000 steps ABNR methods, before starting MD simulations.

Stochastic boundary molecular dynamics (SBMD)²¹ was carried out for 3000 ps using the program CHARMM on structures **A**, **B**, and **C**. For SBMD, a 40 Å reaction zone with a 2 Å buffer region (between 41–42 Å) from the cofactor of subunit A was used. All the enzyme atoms that were at a distance beyond 42 Å from the center of mass were constrained after the minimization. Heavy atoms of the enzyme in the buffer region were constrained using force constants calculated from their average Debye–Waller factors. The system was coupled to a heat bath of 300 K with a frictional coefficient 250 ps⁻¹ on the heavy atoms of enzyme.²¹ The frictional coefficient of buffer region water oxygens was assigned 62 ps⁻¹. A spherical boundary potential generated for 42 Å radius sphere was used.

All atoms within 40 Å of the origin were treated by the ordinary equations of motion using verlet dynamics,²⁴ and those in the buffer zone, by Langevin dynamics. An integration time step of 0.0015 ps and a constant dielectric of unity were used. SHAKE²⁵ was applied to all covalent bonds involving hydrogens. Lennard-Jones interactions were truncated at a distance of 12 Å. A test simulation undertaken on structure **C** has shown that the protonated O5 oxygen of **III** moves farther away from Ca²⁺ (from 2.55 to ~3.70 Å), breaking the coordination. Therefore, during the initial period of dynamics (until 225 ps) a restraint of force constant 50 kcal mol⁻¹ Å⁻¹ was imposed on Ca²⁺⋯O5 separation in structure **C**. After 225 ps the corresponding structure was allowed, without constraints to rearrange according to the CHARMM force field parameters.²²

Since the active sites in both the subunits of sGDH are the same, the analysis was performed only on the trajectories of the subunit A, which is completely in water. The root-mean-square deviation (rmsd) values of the active site were evaluated by least-squares fitting the atoms to the minimized structure. The Ca²⁺, cofactor, and all atoms of the active-site enzyme residues, Gln76, Gly137, Leu138, Asp143, His144, Ser146, Asp163, Gln168, Leu169, Arg228, Asn229, Gln231, Gln246, Gly247, Pro248, Asp252, Tyr343, Trp346, Thr348, Lys377, Arg406, Arg408, and Asp424 were considered for rmsd calculation along with the glucose and glucoactone in structures **A** and **B**, respectively. All the MD structures were averaged during the period 2000–3000 ps for analysis. The molecular and stereo plots were drawn using the programs MOLSCRIPT²⁶ (rendered by Raster3D²⁷) and PyMOL.²⁸

Results and Discussion

Root-Mean-Square Deviations (rmsd). The time variation plot of the rmsd values of the cofactor, Ca²⁺ and the active-site residues of sGDH of the MD structures **A**, **B**, and **C** with respect to the corresponding minimized structure is given in Figure 2.

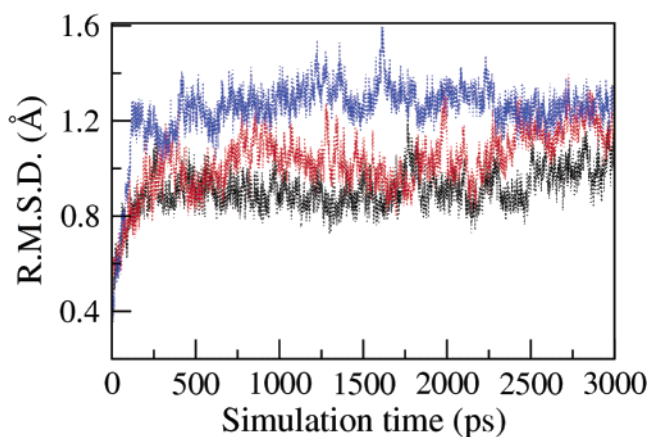


Figure 2. Root-mean-square deviations (rmsd) of the active-site atoms (details mentioned in Methods) of structures **A** (black), **B** (red), and **C** (blue), relative to the corresponding minimized structures during the MD simulation.

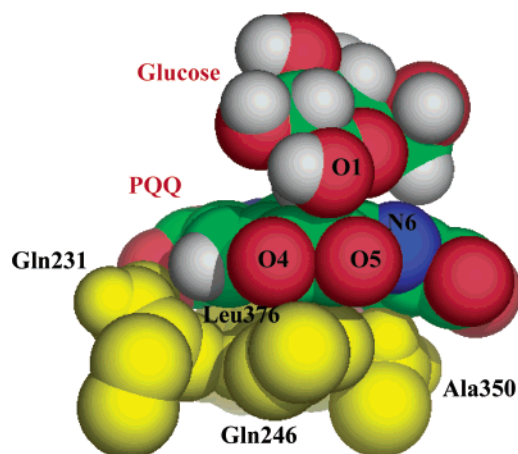


Figure 3. CPK representation of the cofactor PQQ stacked onto the hydrophobic sGDH residues (in yellow) of the MD averaged structure **A**. The substrate glucose is above the plane of PQQ. The carbon, oxygen, and hydrogen atoms of the PQQ and glucose are shown in green, red, and white, respectively, and the nitrogen of PQQ in blue.

The values are slightly higher in intermediate structures **B** and **C** (red and blue lines respectively), compared to the ground-state structure **A** (black line). The values fluctuate within 0.2–0.4 Å in each MD structure. The maximum rmsd value (1.60 Å) is observed for structure **C**.

Active Site of sGDH. The cofactor PQQ resides in a deep, broad positively charged cleft at the top of the barrel near the pseudosymmetry axis (Figure 1). The binding of PQQ to the enzyme is mainly governed by polar interactions, as discussed below. The planar structure of PQQ stacks onto a flat surface area that is largely built up from the side chains of Gln231, Gln246, Ala350, and Leu376 (Figure 3). The binding site of glucose is a wide and solvent-accessible crevice that is located directly above the PQQ. Glucose is held in place at the active site by hydrogen bonding and hydrophobic interactions with PQQ and enzyme. An overview of the active site of the MD structures **A**, **B**, and **C** (Chart 1) are given in stereo plots of Figure 4. The nonbonded distances of interacting atoms at the active site of X-ray and MD averaged (2000–3000 ps) structures are given in Table 1 and Supporting Information, Tables S1–S3.

PQQ Carboxylate Interactions. The interactions of C2, C7, and C9 carboxyl groups of cofactor observed in the MD

(23) Jorgensen, W. L.; Chandrasekhar, J.; Madhura, J. D.; Impey, R. W.; Klein, M. L. *J. Chem. Phys.* **1983**, *79*, 926.

(24) Verlet, L. *Phys. Rev.* **1967**, *159*, 98.

(25) Ryckaert, J. P.; Ciccoliti, G.; Berendsen, H. J. C. *J. Comput. Phys.* **1977**, *23*, 327.

(26) Kraulis, P. J. *J. Appl. Crystallogr.* **1991**, *24*, 946.

(27) Merritt, E. A.; Bacon, J. D. *Methods Enzymol.* **1997**, *277*, 505.

(28) Delano, W. L. *PyMOL: A Molecular Graphics System*, version 0.86; Delano Scientific: San Carlos, CA, 2003.

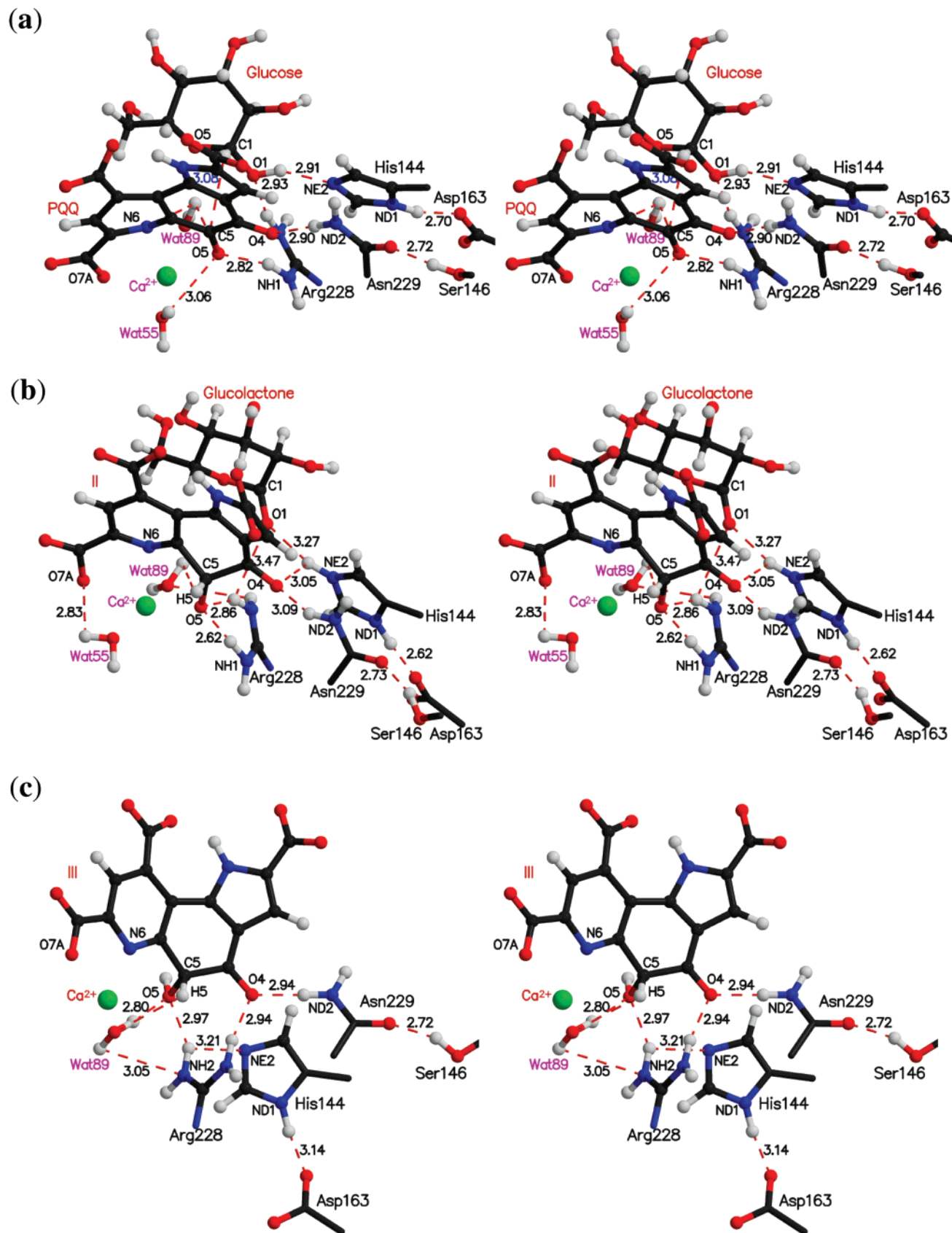


Figure 4. Stereo plots of the active site depicting a few essential residues of the MD averaged structures (a) **A**, (b) **B**, and (c) **C**. Nonbonded interactions are shown by red dashed lines. Average nonbonded distances between heavy atoms are given in Å. In (a) the distance between the C5 of PQQ and H1 of glucose is given in blue.

structures **A**, **B**, and **C** (Supporting Information, Table S1) are almost the same as those seen in the X-ray structure.¹¹ In all

the MD structures the carboxylate oxygen O2B forms bidentate interactions with the guanido nitrogen NH1 of Arg408 and

Table 1. Nonbonded Distances (Å) between Glucose and Other Atoms in the Active Site of the X-ray (1CQ1) and the MD Averaged (2000–3000 ps) Structures (Standard Deviations of the MD Structure Are Given in Parentheses)

Nonbonded distances	X-ray	A
NE2(His144)···O1(glucose)	2.98	2.91 (± 0.17) ^a
NE2(His144)···HO1(glucose)	—	2.05 (± 0.29)
C5(PQQ)···C1(glucose)	3.20	3.60 (± 0.17) ^b
C5(PQQ)···H1(glucose)	—	3.08 (± 0.25)
C5(PQQ)···O1(glucose)	3.58	3.47 (± 0.25) ^a
O5(PQQ)···C1(glucose)	3.42	4.01 (± 0.21)
O5(PQQ)···H1(glucose)	—	3.79 (± 0.30)
O5(PQQ)···O1(glucose)	3.30	3.47 (± 0.25) ^a
O5(PQQ)···HO1(glucose)	—	3.79 (± 0.30)
NE2(Gln76)···O2(glucose)	2.94	3.26 (± 0.28) ^b
OD1(Asp143)···O2(glucose)	2.57	2.78 (± 0.33) ^b
NE2(Gln168)···O1(glucose)	2.71	3.67 (± 0.40)
NH2(Arg228)···O1(glucose)	2.81	2.93 (± 0.16) ^a
O(Wat89)···O5(glucose)	2.82	3.45 (± 0.38)

^a Values within 0.25 Å and different than the crystal structure. ^b Values within 0.26–0.45 Å different than the crystal structure.

amide nitrogen NE2 of Gln231, while O2A hydrogen bonds with NH2 of Arg408. As observed in the X-ray structure, during dynamics the C7 carboxyl group of the cofactor makes hydrogen-bond and ion-pair interactions with Thr348 and Lys377, respectively. A stereo plot showing the equatorial interactions in the active site of structure **C** is given in Figure 5. A novel feature noticed in structure **C** is that the carboxylate oxygen O9A is proximal (2.63 ± 0.10 Å) to the hydroxyl oxygen of Tyr343. The ion-pair interactions of the C9 carboxyl group of cofactor and Arg406 are retained in the MD structures **A**, **B**, and **C**.

Roles of Ca²⁺. sGDH is a homodimer in which the subunits are held together by four calcium ions. In addition, each subunit has a Ca²⁺ at the active site that is ligated, at distances between 2.2 and 2.6 Å (Figure 6a), to two water molecules (Wat55 and Wat89), three functional groups of PQQ, and two functional groups of the enzyme. The PQQ ligands to active-site Ca²⁺ are the pyridine nitrogen N6, C7 carboxylate oxygen

O7A, and C5 quinone carbonyl oxygen O5. The enzyme ligands for Ca²⁺ are main-chain amide carbonyl oxygens of Gly247 and Pro248.

The active-site Ca²⁺ has been suggested to play a role in the polarization of the PQQ C5=O5 bond,^{10,29} enhancing the reactivity of the quinone carbon, C5 toward nucleophiles. As observed in crystal structure¹¹ the heptacoordination of Ca²⁺ is maintained during simulation of structure **A** with average distances between 2.22 ± 0.07 and 2.41 ± 0.13 Å (Figure 6a). However, the coordination of Ca²⁺ is altered in structures **B** and **C**. In structure **B**, Ca²⁺ is hexacoordinated, with the main-chain carbonyl oxygen of Pro248 not ligated after 200 ps of dynamics (Figure 6b). In structure **C** the coordination to the O5 oxygen of **III** is exchanged for a TIP3P water oxygen after 1000 ps of dynamics (Figure 6c). The other ligands of Ca²⁺ in structure **C** are similar to those observed in structure **A**.

Glucose Oxidation. The apparent hydride-transfer mechanism for oxidation of glucose by sGDH (Scheme 1) has been proposed to be assisted by the imidazole of His144 through general base catalysis of abstraction of the proton from the hydroxyl oxygen, O1 at the C1 of glucose.^{10,11,14} The involvement of a functional group with a pK_{app} of ~6 has been offered as support for this proposal. The absolute β-anomer configuration of glucose is the requirement for stereospecific hydride transfer of the H1 at C1 of the glucose to the C5 carbon of PQQ.¹¹ A time variation plot shows that the glucose hydroxyl oxygen of -(H)C1-OH is close (2.91 ± 0.17 Å) to the imidazole nitrogen NE2 of His144 in structure **A** during the entire dynamics (Figure 7a and Table 1). Thus, His144 is positioned to play the vital role of general base to abstract the proton of the hydroxyl O1 group of glucose. Significantly, during most of the simulation, the hydrogen substituent H1 at C1 carbon of glucose approaches the quinone carbonyl carbon C5 of PQQ (3.08 ± 0.17 Å) sufficiently for hydride or equivalent transfer (Figures 7b and 3a).

Role of His144. In the average MD structures of **A**, **B**, and **C**, the imidazole nitrogen, NE2 of His144 is at a distance 3.46,

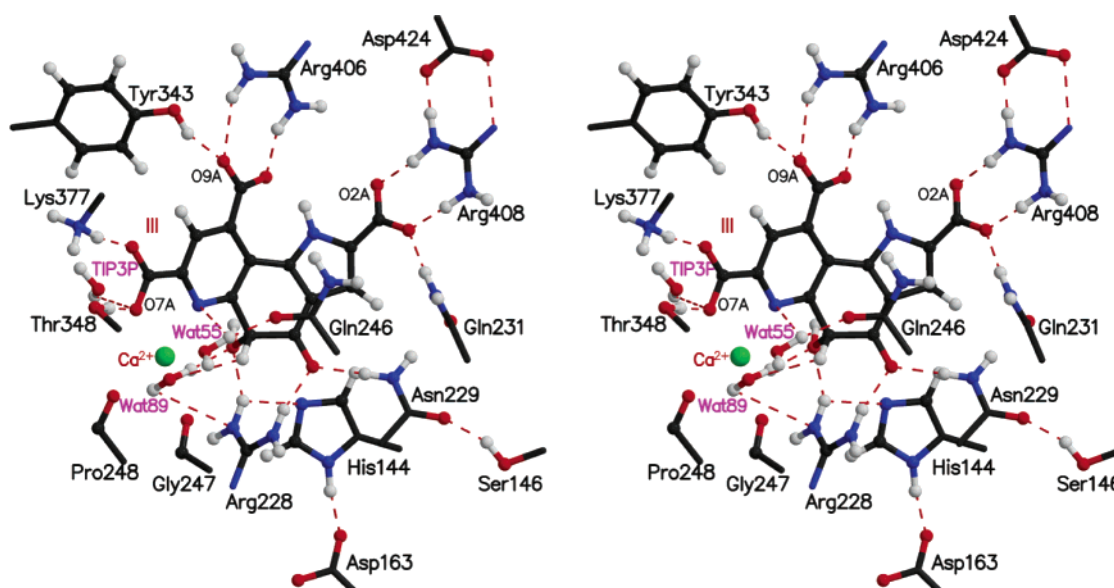


Figure 5. Stereo plot of the equatorial hydrogen-bond and ion-pair interactions in the active site of the MD averaged structure **C**. The nonbonded interactions are shown by red dashed lines. For clarity Asp252 that hydrogen bonds to Wat55 is omitted. The corresponding distances are provided in the Supporting Information, Tables S1–S3.

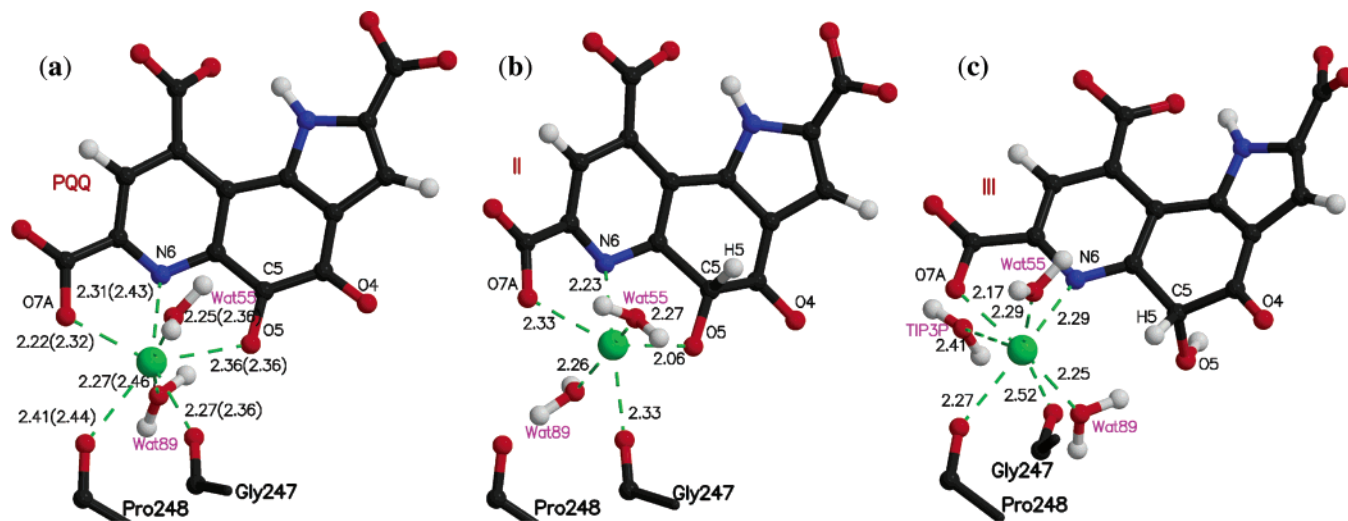


Figure 6. The Ca^{2+} (green) coordination in the MD averaged structures (a) **A**, (b) **B**, and (c) **C**. The coordinating distances are in Å. In (a) values of the X-ray structure are given in parentheses. Observe in (b) Pro248 is no longer ligated to Ca^{2+} . Also, in (c) ligation of the O5 oxygen of **III** to Ca^{2+} is replaced by a TIP3P oxygen.

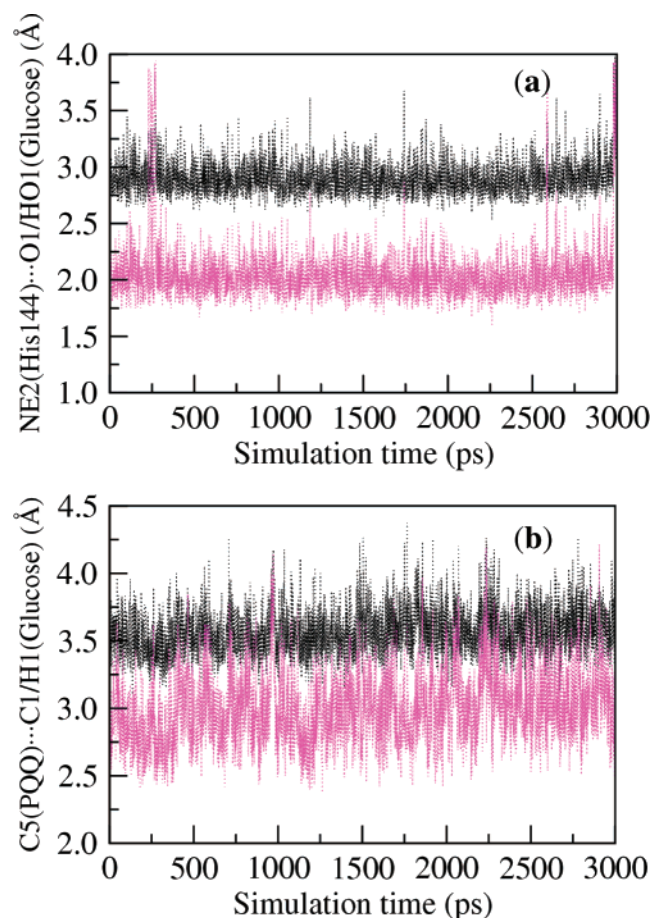


Figure 7. Time-dependent variation of separation of the (a) imidazole nitrogen NE2 of His144 and oxygen O1 (black)/hydrogen H01 (pink) at the C1 of glucose; (b) quinone carbonyl carbon C5 of PQQ and glucose carbon C1 (black)/hydrogen H1 (pink) of the MD structure **A**.

3.40, and 3.21 Å, respectively to the guanido nitrogen, NH2 of Arg228 (Figure 4 and Supporting Information, Table S2). As also seen in the crystal structure,¹¹ the δ nitrogen ND1 makes a stable hydrogen bond with a carboxylate oxygen of Asp163. The Asp163- CO_2^- , the imidazole of His144, and the hydroxyl

oxygen O1 of glucose form a triad, which is stabilized by strong hydrogen bonds (2.70 and 2.91 Å), a feature analogous to Asp-His-Ser triad of serine proteases.³⁰

It has been suggested^{10,14} that the imidazolium of His144 in structure **B**, donates a proton to the oxyanion O5 of **II** (Scheme 1). However, during the MD simulation, this required interaction is not observed since the O5 of **II** is engaged in hydrogen-bond interactions with Arg228 (2.62 ± 0.08 and 2.86 ± 0.23 Å) and Wat89 (3.14 ± 0.18 Å) (Figure 4b). Noticeable in structure **B** is that the protonated NE2 of His144 forms a hydrogen bond (3.05 ± 0.23 Å) with the O4 carbonyl oxygen of **II**. Thus, protonated His144 is in a position to be proton donor to $>\text{C4}=\text{O}$. Also NE2 of His144 is proximal (3.27 ± 0.55 Å) to the O1 oxygen of the glucolactone product.

His144 has been suggested^{10,14} to play the role of general base in migration of the H5 hydrogen of **III** (Scheme 1) to provide the hydroquinone PQQH₂ in structure **C**. This role for His144 is unlikely because the NE2 of His144 is too far (4.82 ± 0.25 Å) from the H5 of **III** (Figure 8a and Supporting Information, Table S2).

Interactions of Arg228 and Asn229. Arg228 is positioned in the active site such that it polarizes the C5–O5 bond of the cofactor. In structure **A** the O5 oxygen of PQQ forms a hydrogen bond (2.82 ± 0.12 Å) with the guanido nitrogen NH1 of Arg221 (Supporting Information, Table S2), while in structure **B**, the oxyanion O5 of **II** is involved in bidentate electrostatic interactions with the guanido moiety of Arg228 (Figure 4, a and b). In structure **C**, besides the hydrogen-bond interaction between O5 of **III** and NH2 of Arg228 (2.97 ± 0.18 Å), the carbonyl oxygen O4 of **III** and guanido nitrogen NH1 of Arg228 are proximal (2.94 ± 0.15 Å), forming a strong hydrogen bond (Figure 4c). These interactions of Arg228 would have a positive influence on the hydroquinone formation. The amide nitrogen ND1 of Asn229 forms a stable hydrogen bond with the O4, carbonyl oxygen of cofactor in structures **A**, **B**, and **C** (Figure 4). The position of Asn229 is stabilized by hydrogen-bond interactions with the hydroxyl oxygen of Ser146 in the MD structures, as in the X-ray structure.¹¹

(29) Zheng, Y.-J.; Bruce, T. C. *Proc. Natl. Acad. Sci. U.S.A.* **1997**, *94*, 11881.

(30) Dodson, G.; Wlodawer, A. *Trends Biochem. Sci.* **1998**, *23*, 347.

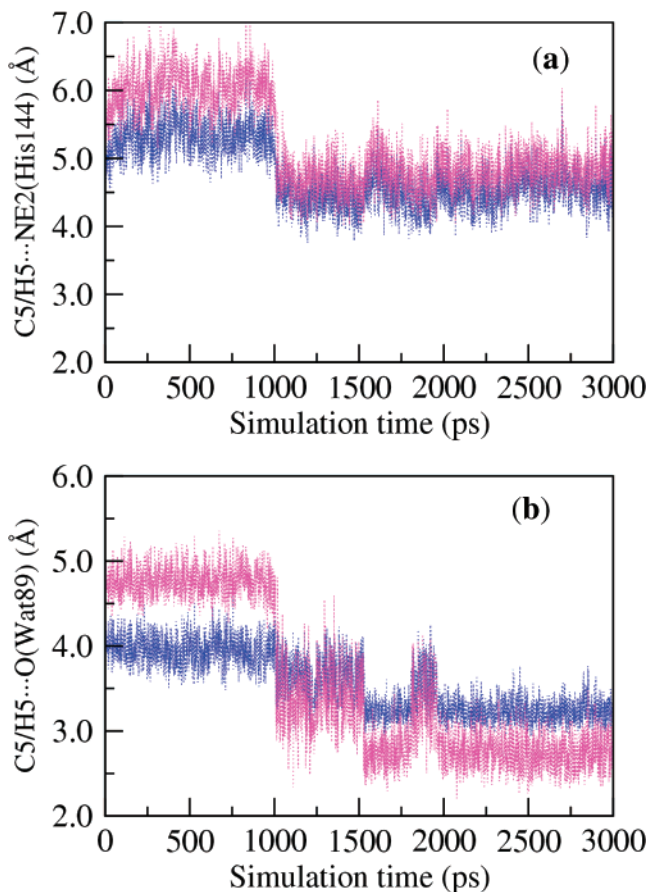
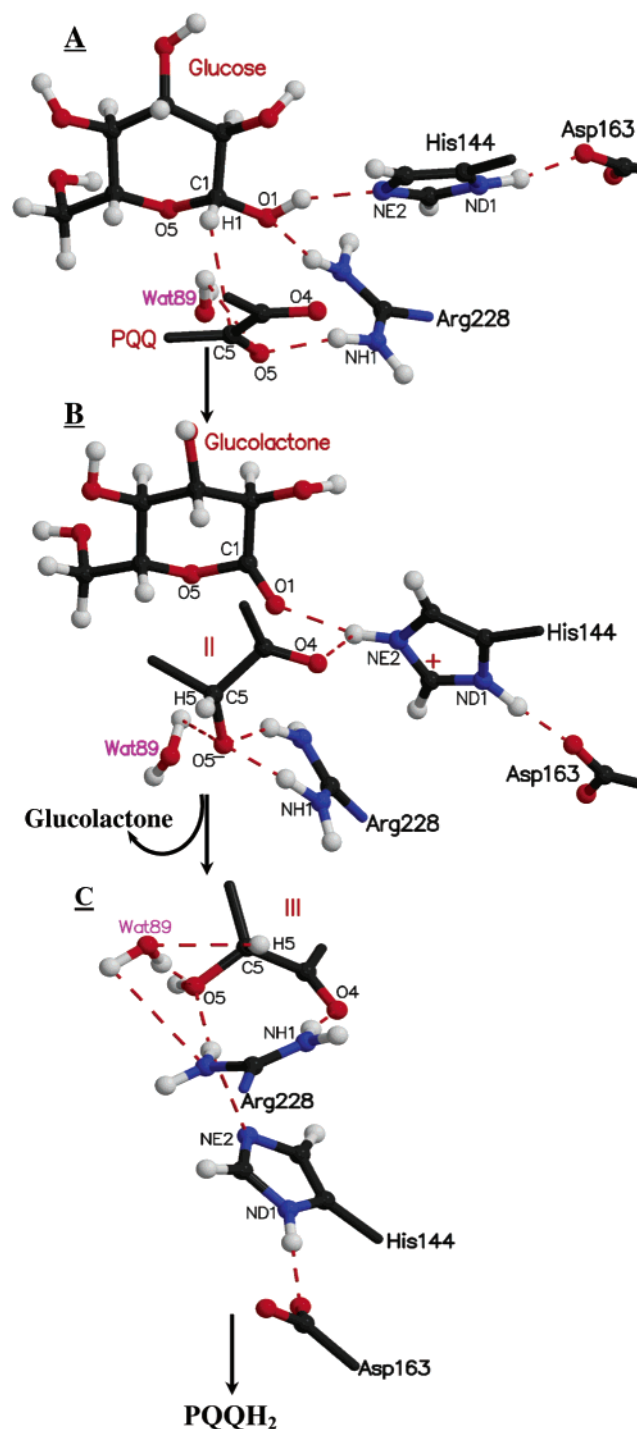


Figure 8. Time-dependent variation of separation of the C5 carbon (blue)/H5 hydrogen (pink) of **III** with (a) the imidazole nitrogen NE2 of His144 and (b) crystal water Wat89 oxygen of the MD structure **C**.

Motions of Waters. Of the several crystal waters, Wat55 and Wat89 are in the active site ligated to Ca^{2+} and engaged in interactions with the cofactor and also with active-site residues of the enzyme. In structure **A**, Wat55 is hydrogen bonded to the $>\text{C5}=\text{O}$ oxygen of PQQ (Figure 4a) as well as side-chain oxygens of Asp252 and Gln246 (Supporting Information, Table S3). In structures **B** and **C**, Wat55 moves farther away from the O5 of cofactor but makes a hydrogen bond with the $-\text{CO}_2^-$ at C7 of **II** and N6 of **III** (Figure 4, b and c). A stable hydrogen bond between Wat55 and the carboxylate oxygen OD1 of Asp252 is also seen in structures **B** and **C**.

In structure **A**, Wat89 is hydrogen bonded to the N6 and O5 of PQQ (2.99 ± 0.11 and 2.91 ± 0.14 Å, respectively), main-chain oxygen of Pro248 (2.88 ± 0.13 Å) and guanido nitrogen NH2 of Arg228 (3.33 ± 0.22 Å) (Figure 4a). Similar interactions are observed in structure **B**, except that hydrogens of Wat89 are pointing away from the N6 of **II**. According to the MD structure **C**, any rearrangement of $-(\text{H})\text{C5}(\text{OH})-\text{C4}(=\text{O})-$ to the PQQH₂ hydroquinone, $-\text{C5}(\text{OH})=\text{C4}(\text{OH})-$ would be assisted by two hydrogen bond networks. These involve Wat55 and Wat89 through Asp252, Gln246, and Arg228 and His144 (Supporting Information, Figure S1). A time variation plot shows that Wat89 is proximal (2.74 ± 0.19 Å) to the H5 at the tetrahedral C5 of **III** after 2000 ps of dynamics (Figure 8b). This suggests that Wat89 would be involved in departure of the C5 hydrogen of **III** if this species should be intermediate to PQQH₂. This is an interesting feature not suggested by X-ray studies.¹¹

Chart 2



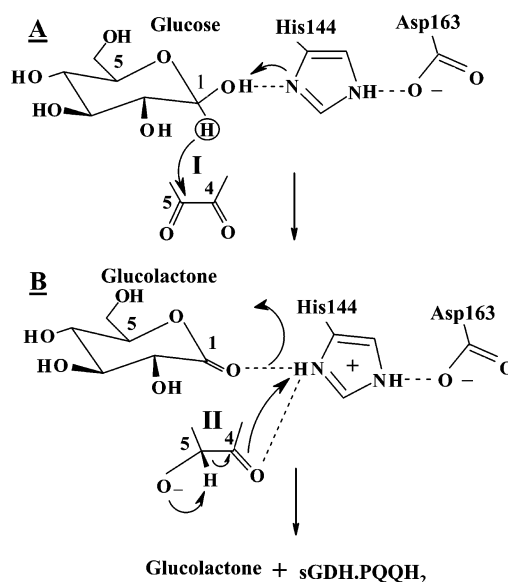
Conclusions

Procedures that were involved in determining the X-ray coordinates employed as the basis for the present study involved soaking of the crystals of the apo-enzyme in a PQQ-containing solution and subsequently in a solution with glucose. Oubrie and co-workers¹¹ interpreted the resultant structure to contain the reduced PQQ and glucose. However, it is hard to differentiate between the oxidized and reduced forms of PQQ on the basis of the X-ray studies. In such cases MD studies are useful to provide insights into the catalytic mechanism of the enzyme with the visible hydrogens and explicit inclusion of water.

The three MD structures examined, **A**, **B**, and **C** are characterized by hydrogen bonding of Arg228 to the C5 oxygen functions of **I**, **II**, and **III** and Asn229 to the $>C4=O$ oxygen. The mechanism for PQQ reduction by methanol in the quinoprotein methanol dehydrogenase (MDH) is also aided by hydrogen bonding of arginine (Arg324) to the PQQ $>C5=O$ and $>C4=O$ oxygens.^{31–34} Also, the methanol dehydrogenase reaction involves hydrogen bonding between $>C4=O$ oxygen and an amide side chain of Asn387, which is also observed in the MD structures of sGDH (with respect to Asn229). The pattern of Ca^{2+} coordination to PQQ ligands in the intermediate structures (**II** and **III**) of sGDH and MDH obtained from MD simulations are analogous.^{33,34}

The structures related to the mechanistic steps of glucose oxidation of sGDH via PQQ reduction are given in Chart 2. The His144, as previously suggested by X-ray study,¹¹ is most likely a general base catalyst in PQQ reduction. The general base catalysis is associated with the tight hydrogen bonds of the Asp163-His144-glucose triad (2.70 and 2.91 Å). This geometry and increase of quinone oxidation potential by hydrogen bonding of $>C5=O$ of PQQ with Arg228 allows a concerted reaction. The immediate product from glucose oxidation is glucolactone, which interacts with Arg228 and His144 of sGDH. Hydride transfer to $-C5(=O)-C4(=O)-$ of PQQ leads to $-(H)C5(O^-)-C4(=O)-$ of **II**. The formation of **II** in structure **B** is assisted by bidentate hydrogen-bond interactions of Arg228 to the oxyanion O5 of **II**. In structure **B**, the average distance from the O5 of **II** to the protonated His144 is 4.79 Å. Thus, protonation of the oxyanion entity of **II** by His144, as suggested by X-ray studies (Scheme 1),¹¹ is not possible. Also, the positioning of His144 to be a general base catalyst for proton abstraction from **III** in structure **C** is not favorable. However, Wat89 is in position to play a role in solvation of this proton formed from $C5-H$, departing from $>(H)C5(OH)$ region of **III** to provide the hydroquinone $PQQH_2$. This is an exothermic

Chart 3



reaction due to creation of an aromatic system. Thus, the weak base Wat89 would suffice to solvate the leaving proton.

Alternately a spontaneous conversion of **II** \rightarrow $PQQH_2$ (Chart 3) with protonated His144 hydrogen bonded to the $>C4=O$ of **II** playing the role of general acid catalyst must be considered. Glucolactone dissociation from the enzyme would occur where the hydrogen bonding to the protonated His144 is no longer possible.

Acknowledgment. The work was supported by the NIH Grant (5R37DK0917138). The authors acknowledge computer time on UCSB's SGI Origin 2000 and at NPACI Supercomputer Center.

Supporting Information Available: Figure S1 (active site of the MD averaged structure **C**), Tables S1, S2, and S3 (non-bonded distances (Å) of the active site residues of the X-ray and MD averaged structures) (PDF). This material is available free of charge via the Internet at <http://pubs.acs.org>.

JA039722R

(31) Xia, Z.-x.; He, Y.-n.; Dai, W.-w.; White, S. A.; Boyd, G. D.; Mathews, F. S. *Biochemistry* **1999**, *38*, 214.

(32) Zheng, Y.-J.; Xia, Z.-x.; Chen, Z.-w.; Mathews, F. S.; Bruice, T. C. *Proc. Natl. Acad. Sci. U.S.A.* **2001**, *98*, 432.

(33) Reddy, S. Y.; Bruice, T. C. *J. Am. Chem. Soc.* **2003**, *125*, 8141.

(34) Reddy, S. Y.; Mathews, F. S.; Zheng, Y.-J.; Bruice, T. C. *J. Mol. Struct.* **2003**, *655*, 269.